ELSEVIER

Journal of Alloys and Compounds 330–332 (2002) 747–751

Journal of ALLOYS AND COMPOUNDS

www.elsevier.com/locate/jallcom

Effect of mechanical grinding under Ar and H_2 atmospheres on structural and hydriding properties in $LaNi_5$

H. Fujii[a,*], S. Munehiro[b], K. Fujii[b], S. Orimo[a]

[a]*Faculty of Integrated Arts and Sciences, Hiroshima University, 1-7-1 Kagamiyama, Higashi-Hiroshima 739-8521, Japan*
[b]*Eastern Hiroshima Prefecture Industrial Research Institute, Fukuyama 721-0974, Japan*

Abstract

The effects of mechanical grinding (MG) under argon and hydrogen gas atmospheres on the hydrogen storage properties of a $LaNi_5$ alloys were studied in detail. During MG under Ar atmosphere, a crystallite size reaches a ~20 nm in grinding time of 60 min and reduces to approximately half this size after 600 min without any dissociation. The pressure–composition isotherm (P–C) in $LaNi_5$ at 293 K indicates an increase in hydrogen in zero offset region (trapping site region), a lowering of plateau pressure and a narrowing of the width of the pressure plateau by MG. On the other hand, in reactive MG (RMG)-$LaNi_5$ under H_2 atmosphere, a nanocrystalline $LaNi_5H_{0.15}$ and an amorphous phase coexist when the grinding time is less than 180 min. For much longer RMG times than 180 min, the nanostructured $LaNi_5H_{0.15}$ phase disappears and the remaining amorphous phase dissociates into nanocrystalline Ni + amorpous $LaNi_yH_z$ ($y<5$). The P–C isotherm indicates no plateau for the $LaNi_5$ produced by RMG longer than 60 min and the hydriding properties become worse and worse with increasing RMG times. From the above results, we conclude that the hydriding properties cannot be improved by structural modifications in systems containing metals with a strong affinity for hydrogen like rare earth metals.

Keywords: Hydrogen storage; Nano-structured $LaNi_5$; Mechanical grinding; P–C isotherm

1. Introduction

Hydrogen-absorbing materials are attractive as functional materials for rechargeable batteries, movable hydrogen storage tanks, and heat pumps. However, most hydrides have either excellent kinetic properties but a rather low storage capacity by weight, or the few that have higher srorage capacity have very poor kinetics. For achieving high performance for hydrogen storage, so as to have hydrogen capacities higher than 3 mass% and to desorb hydrogen at temperatures lower than 373 K, some non-conventional methods are now in progress; (1) formation of nano-structured and/or amorphous metal hydrides by mechanical grinding or melt-qenching methods [1–5], (2) employment of reversible dissociation reactions in Ti-doped alkali metal aluminium systems [6], (3) improvement of V-based solid solution alloys with bcc crystal structure [7,8] and (4) utilization of carbon-related materials with specific nanometer-scale structures [9–12].

Until now, hydriding properties of some nano-structured Mg–Ni alloys produced by mechanical grinding/alloying have been studied by Zaluski et al. [1,4] and independently by Orimo and co-workers [2,3,5], and it has been clarified that Mg–Ni alloys show changes to their hydriding properties as a result of their modified structures in nanometer-scale. The report concerned with the hydriding properties of nano-structured Mg_2Ni alloy with almost equal volume fraction of nano-crystallite (intra-grain) regions and grain boundary (inter-grain) regions [3]. The existence of the inter-grain regions led to superior hydriding properties in a nano-Mg_2Ni alloy such as the appearance of enhanced hydrogen dissolution and dehydriding at lower temperature than 140°C. The other report was concerned with amorphous MgNi alloy, in which the maximum hydrogen capacity is ~2.2 mass% corresponding to a formula of $MgNiH_{1.9}$, and the dehydriding reaction occurs below 373 K in an argon atmosphere [5]. The electrochemical P–C curve at room temperature indicated the existence of the miscibility-gap pressure, being different from the other amorphous hydrides.

On the other hand, hydriding properties of nano-structured FeTi alloys produced by mechanical grinding (MG) were studied by Zaluski et al. [4]. These showed superior hydrogen absorption–desorption kinetics with no need for

*Corresponding author. Tel.: +81-824-24-6551; fax: +81-824-24-0757.

E-mail address: hfujii@hiroshima-u.ac.jp (H. Fujii).

0925-8388/02/$ – see front matter
PII: S0925-8388(01)01508-0

prior activation, but no good pressure–composition (P–C) isotherm at room temperature with a narrowing of the width of the plateau pressure due to an enhancement of hydrogen solubility and a lowering of plateau pressure. Namely, the thermodynamic hydriding properties in FeTi alloys could not be improved by structural modification on the nanometer scale. Systematic studies concerning with hydriding properties in nano-structured $LaNi_5$ have not been reported yet.

In this work, we have studied the structural and hydrogen absorption–desorption properties of nano-structured $LaNi_5$ produced by MG in Ar and reactive-mechanical grinding (RMG) in hydrogen gas atmospheres, respectively. The purpose of this work is to clarify whether or not the hydriding properties in a typical $LaNi_5$ alloy are improved or not by structural modification on the nanometer scales.

2. Experimental procedures

The $LaNi_5$ sample used in this work was prepared by induction melting and was supplied by Japan Metals & Chemicals. Both the initial compound, 1 g, ~300 μm in size, and 20 steel balls of 7 mm in diameter (weight ratio 1:30) were put in a steel vial 30 cm^3 in volume. The vial was equipped with a connection valve for evacuation or introduction of Ar or hydrogen gas without exposing the sample to air. Prior to grinding, the vial was directly degassed for 720 min (12 h) at less than 0.01 Pa. Then, in the case of MG (RMG) treatments, argon (hydrogen) gas with purity of 7 N was introduced into it up to 1 MPa. The intial compound was mechanically ground using a planetary ball mill apparatus (Fritsch P7) with 400 rpm for periods from 5 to 600 min (10 h) at room temperature.

The products after MG (RMG) treatments were carefully handled in a glove box filled with purified argon to minimize oxidation. The structural properties of the products obtained were examined by X-ray diffraction measurement with Cu Kα radiation. The thermal analyses (thermogravimetry (TG) and differential thermal analysis (DTA)) were carried out under a purified argon atmosphere by heating at 5 K/min up to 950 K. The measurement of pressure (P)–composition (C) isotherms (P–C isotherm) was done at 293 K under hydrogen gas pressures of 0.005–4.0 MPa after several activation cycles. Each data point was taken after 30 min corresponding to the time when it reaches equilibrium.

3. Experimental results

3.1. Effect of MG and RMG on the structural modification

In order to examine how the structure of $LaNi_5$ does change by MG under Ar or RMG under H_2–gas atmospheres, we compared the structural properties of the products obtained by MG with RMG treatments. Figs. 1 and 2 show X-ray diffraction (XRD) profiles at various grinding times for the products prepared by MG and RMG, respectively. From Fig. 1, we can see that the initial compound is a single phase of $CaCu_5$-type structure, but the peak width is made broader with increasing the MG time in Ar atmosphere without any dissociation. From the broadening, we can estimate the crystallite size using the Scherrer equation [13], the size of which is ~20 nm for the product prepared by MG for 60 min and reduces to approximately half this size after 600 min.

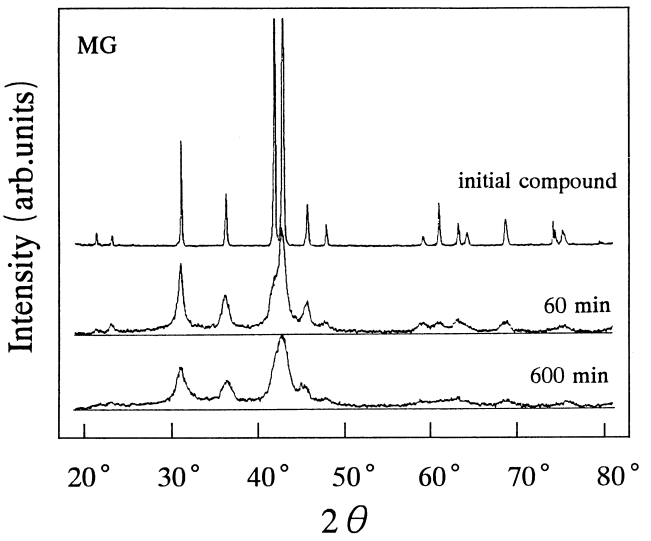

Fig. 1. X-ray diffraction profiles (Cu Kα) of initial $LaNi_5$ compound and modified $LaNi_5$ after MG for 60 min and 600 min.

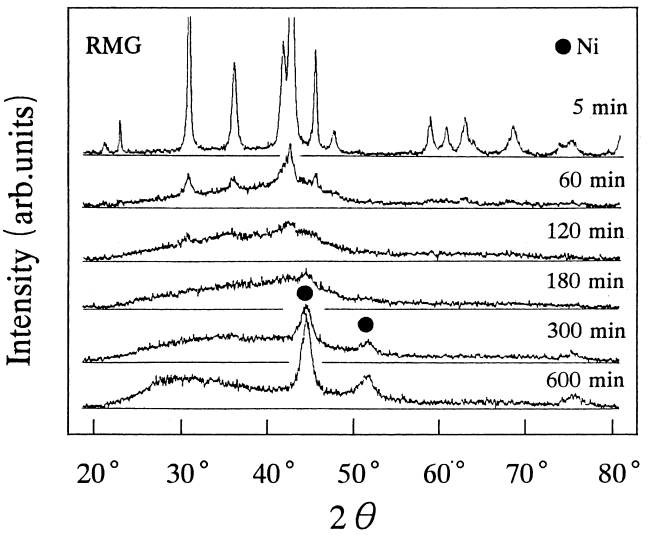

Fig. 2. X-ray diffraction profiles (Cu Kα) of modified $LaNi_5$ after RMG for 5, 60, 120, 180, 300 and 600 min.

On the other hand, for the products prepared by RMG under H_2 gas pressure of 1 MPa, the XRD profiles in Fig. 2 indicate that (1) a small shift of peak position to low angle appears under RMG for 5 min, from which the formation of $LaNi_5H_{0.15}$ was inferred from measurement of mass reduction with increasing temperature by TG. (2) Broadening of the diffraction peaks is strongly promoted with increasing the RMG time up to 180 min, and additionally a broad peak around $2\theta = 40–50^\circ$ grows, suggestive of the appearance of an amorphous phase. Unfortunately, for the products prepared by RMG, we could not estimate the crystalline size because of superposition of two-phase peaks of amorphous and crystalline phases. (3) Beyond 180 min, elemental Ni peaks due to dissociation of $LaNi_5H_x$ appear and they grow with further increase in the RMG time; and (4) the broad peak corresponding to amorphous phase shifts to the low angle side with further increase in the RMG time.

Two models explaining the dissociation of $LaNi_5H_x$ have been so far proposed by Cohen and co-workers [14–16] and Ahn and Lee [17]. The one is that $LaNi_5H_x$ dissociates into LaH_2 and Ni during repeated the hydrogen absorption–desorption cycles [14–16]. The other is that $LaNi_5H_x$ dissociates into $LaNiH_{3.6}$ and Ni by repeated cycles [17]. However, in the RMG treatment, we did not observed LaH_2 or $LaNiH_{3.6}$ in the X ray profiles (see Fig. 2). Therefore, our results must be explained by a different model. The results obtained here could be explained by the following process: (1) at the first step (grinding time $t<5$ min), RMG leads to the formation of $LaNi_5H_{0.15}$; (2) as the next step (5 min$<t<$180 min), an amorphous phase of $LaNi_5H_x$ appears and the phase develops at the same time as $LaNi_5H_{0.15}$ is modified into nano-structure; (3) at $t=$ 180 min, almost all of the sample has become the amorphous $LaNi_5H_x$; (4) as the third step (180$<t<$300 min), a part of the amorphous phase dissociates into another amorphous $LaNi_yH_x$ (y is likely to be equal or close to zero) and nano-crystalline Ni because La is so high affinity for hydrogen (see Table 1) that the H atoms locate near La atoms during longer RMG and Ni atoms are condensed; and (5) at the final step (300$<t<$600 min), the broad peak characteristic of the amorphous phase shifts to low angle side with increasing the amount of Ni segregation, suggesting that the amorphous $LaNi_yH_x$ is gradually transformed into more stable amorphous phase like a-LaH_2 with increasing RMG time [18].

Table 1
Enthalpy change due to hydride formation for the Mg and La systems

Hydride formation	Enthalpy change for formation, ΔH (kJ/mol H_2)
$Mg \rightarrow MgH_2$	74.5
$Mg_2Ni \rightarrow Mg_2Ni_4$	64.4
$La \rightarrow LaH_2$	207.5
$LaNi_5 \rightarrow LaNi_5H_6$	31.8

3.2. Pressure–composition (P–C) isotherm of the products prepared by MG and RMG

The *P–C* isotherms of the products prepared by MG and RMG-treatments were measured at 293 K to reveal how the thermodynamic properties are changed by structural modifications due to MG and MRG. The results obtained after several activation cycles are given in Figs. 3 and 4, respectively. We can see that $LaNi_5$ without any structural modification exhibits the similar *P–C* isotherm as in the literature. The *P–C* isotherm is critically changed by making $LaNi_5$ nanocrystalline by MG as follows: (1) the amount of hydrogen in the zero offset range (trapping site region) increases with increasing the MG time, which is due to absorption in grain boundary sites. Since these do not desorb at the absorption temperature 293 K, they may be referred to as trapping sites near La atoms in them. (2) The width of the pressure plateau is made narrower with increasing the MG time, which is also due to the increase in the amount of inter-grain region. (3) The lowering of the plateau pressure occurs due to MG. Similar results have been reported in an FeTi alloy by Zaluski et al. [4].

In Fig. 4, the *P–C* isotherms for $LaNi_5$ prepared by RMG are shown at 293 K. The characteristic features obtained are summarized as follows. (1) The RMG treatment before dissociation ($t<$180 min) leads to a more rapid decrease in total hydrogen storage capacity and effective (available) hydrogen content, and a more rapid loss of flatness in plateau pressure than in the case for MG.

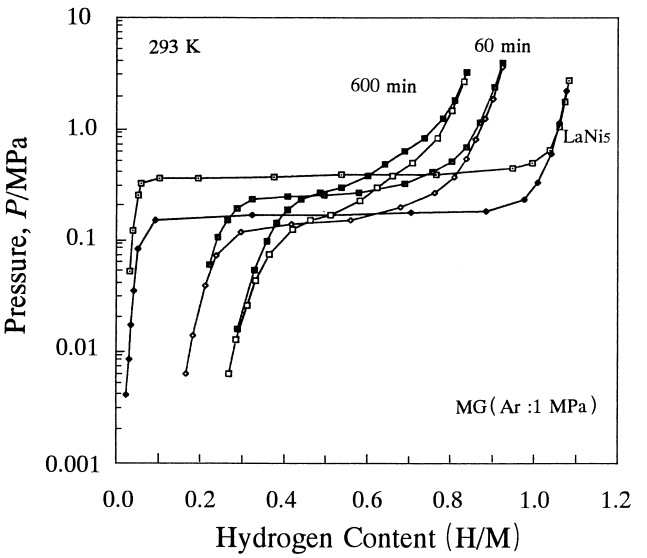

Fig. 3. Hydrogen pressure–composition (*P–C*) isotherms of the initial $LaNi_5$ compound and modified $LaNi_5$ after MG for 60 and 600 min at 293 K. The data were taken after several activation cycles.

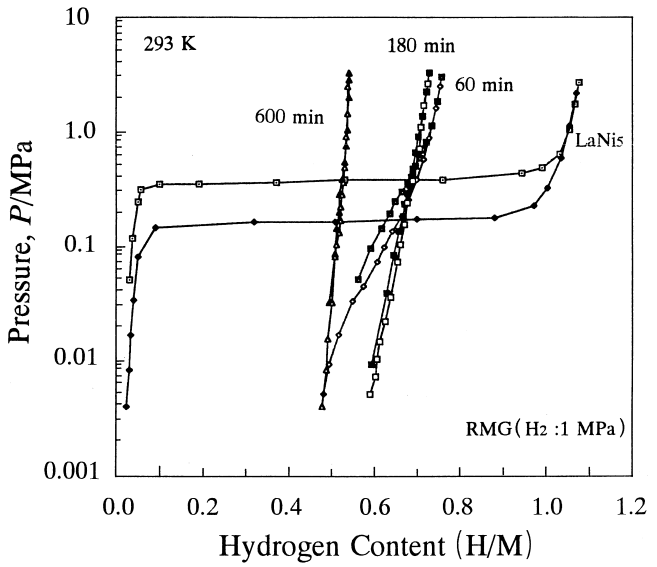

Fig. 4. Hydrogen pressure–composition (P–C) isotherms of the initial $LaNi_5$ compound and modified $LaNi_5$ after RMG for 60, 180 and 600 min at 293 K. The data were taken after several activation cycles.

This disadvantage for hydrogen storage is due to the development of the amorphous phase $LaNi_5H_x$ with increasing RMG time. (2) With further increase in RMG time ($t>180$ min), the total hydrogen storage capacity and the remaining hydrogen content with no desorption at 293 K further decreases with increase in Ni content. The further decrease in total hydrogen content can be understood by the complete decomposition of the $LaNi_5$ (Ref. Fig. 2).

The hydrogen concentration which is not desorbed at 293 K under equilibrium condition rapidly increases by increase in the MG and RMG times. The thermal stability for the trapped hydrogen can be estimated by the DTA measurement. In the DTA profiles of $LaNi_5H_x$ after measuring the P–C isotherms, a single exothermic peak at 340 K appeared for the MG-$LaNi_5$, and for RMG-$LaNi_5$ without Ni segregation prepared by shorter grinding than 180 min. On the other hand, the DTA profile in RMG for grinding times longer than 180 min showed two peaks. Therefore, from the those results, we can deduce the existence of the following three hydrogen occupation sites: in the case of MG treatment (1) the first site is the intra-grain site in nanostructured $LaNi_5$, where hydrogen can absorb and desorb at 293 K under equilibrium condition. (2) The second site is the inter-grain (grain boundary) site formed by MG, in which the atomic arrangement is random and disordered. This kind of hydrogen can desorb at 340 K. (3) In the case of RMG treatment, the third sites are in the amorphous phase $LaNi_y$ (y is likely to be equal or close to zero), which is formed with the appearance of Ni due to the dissociation of $LaNi_5H_x$ by longer RMG than 180 min. However, the site (1) is largely inactive after RMG for 180 min as shown in Fig. 4. The hydrogen in (3) might be desorbed at 540 K, which was observed in the DTA profile.

4. Discussion

From the above experimental results, we can conclude that nanostructural modifications due to MG under Ar and RMG under H_2 gas pressure of 1 MPa do not lead to any suitable improvement of the thermodynamic hydriding properties in $LaNi_5$; however, an improvement in the kinetics was observed. This conclusion is in contrast with that in Mg_2Ni, in which the hydriding properties were remarkably improved by RMG in H_2 gas atmosphere. This contrasting behavior could originate in the difference in the formation enthalpies between the Mg and La systems. In Table 1, the enthalpy change due to hydride formation ΔH for the Mg and La systems [19] is given. All the systems could form stable hydrides because of negative and large ΔH for all the metals and compounds. However, we notice that for the Mg system, the difference of ΔH of formations for MgH_2 and Mg_2NiH_4 is small, while that for the formations of LaH_2 and $LaNi_5H_6$ is quite large, indicating that LaH_2 is very stable compared with $LaNi_5H_6$. Generally, it has been claimed that the volume fraction of inter-grain regions becomes comparable to that of the intra-grain (crystallite) regions by structural modification into nanometer scales due to MG or RMG. Therefore, if hydrogen is induced in inter-grain regions in $LaNi_5$, the hydrogen is located near La atoms because of strong affinity for hydrogen and forms a much more stable hydride than $LaNi_5H_6$. Since the hydrogen capacity in the inter-grain regions is smaller than that in the crystallite $LaNi_5H_6$ and the hydrogen does not contribute to absorption–desorption cycles at room temperature, the MG treatment leads to an increase of hydrogen in zero offset region in the P–C isotherm. Conversely, the volume fraction of the $LaNi_5$ crystallite regions is decreased by nanostructural modification. Accordingly, the total hydrogen storage capacity is decreased by MG. In the case of RMG-$LaNi_5$, since the amorphous phase $LaNi_5H_x$ is easily formed by RMG, hydrogen is preferentially located near La atoms and the structure of $LaNi_5H_x$ locally dissociates into $LaNi_yH_z$ ($y<5$) and Ni. Such modifications lead to worse hydriding properties in this system.

Zaluski et al. [4] have studied the effect of MG on the hydriding properties in TiFe alloy. They also observed an improvement of kinetics, an enhancement of hydrogen solubility, a lowering of plateau pressure and a narrowing of width of plateau by MG. These results could also have originated in the large difference of ΔH for formations of TiH_2 and $TiFeH_2$. On the other hand, in the case of Mg_2Ni, since the difference of ΔH in formations of MgH_2 and Mg_2NiH_4 is small, it seems that the structure of Mg_2Ni and the atomic distribution do not change by MG and RMG. This might lead to the appearance of the

remarkable hydriding properties in nano-structured Mg_2Ni produced by RMG [2,3].

In conclusion, We cannot expect any improvement in hydriding properties of $LaNi_5$ by structural modification into nanometer size, because the inter-grain (grain boundary) region leads to formation of too stable hydride in the system containing rare earth metals like La with strong affinity for hydrogen.

Acknowledgements

This work was supported by Funds of the Japan Science and Technology Corporation and Research Development of Hiroshima Prefecture, and a Grant-in-Aid for Scientific Research on Priority Area A of 'New Protium Functions' from the Ministry of Education, Science and Culture, Japan.

References

[1] L. Zaluski, A. Zaluska, J.O. Ström-Olsen, J. Alloys Comp. 217 (1995) 245.
[2] S. Orimo, H. Fujii, J. Alloys Comp. 232 (1996) L16.
[3] S. Orimo, H. Fujii, K. Ikeda, Acta Mater. 45 (1997) 331.
[4] L. Zaluski, A. Zaluska, J.O. Ström-Olsen, J. Alloys Comp. 253–254 (1997) 70.
[5] S. Orimo, K. Ikeda, H. Fujii, S. Saruki, T. Fukunaga, A. Züttel, L. Schlapbach, Acta Mater. 46 (1998) 4519.
[6] B. Bodganovic, M. Schwickardi, J. Alloys Comp. 253–254 (1997) 1.
[7] H. Iba, E. Akiba, J. Alloys Comp. 253–254 (1997) 21.
[8] T. Kuriiwa, T. Tamura, T. Amemiya, T. Fuda, A. Kamegawa, H. Takamura, M. Okada, J. Alloys Comp. 293–295 (1999) 433.
[9] A.C. Dillon, K.M. Jones, T.A. Bekkedahl, C.H. Kiang, D.S. Bethune, M.J. Heben, Nature 386 (1997) 377.
[10] A. Chambers, C. Park, R. Terry, K. Baker, N.M. Rodorigues, J. Phys. Chem. B 102 (1998) 4253.
[11] C.C. Ahn, Y. Ye, B.V. Ratnakumar, C. Witham, R.C. Bowman Jr., B. Fulz, Appl. Phys. Lett. 73 (1998) 3378.
[12] S. Orimo, G. Majer, T. Fukunaga, A. Züttel, L. Schlapbach, H. Fujii, Appl. Phys. Lett. 75 (1999) 3093.
[13] B.D. Cullity, in: Elements of X-ray Diffraction, Addison-Wesley, Reading, MA, 1977.
[14] R.L. Cohen, K.W. West, J.H. Wernick, J. Less-Common Met. 70 (1980) 229.
[15] R.L. Cohen, K.W. West, J.H. Wernick, J. Less-Common Met. 73 (1983) 273.
[16] R.L. Cohen, K.W. West, J. Less-Common Met. 95 (1983) 17.
[17] H.J. Ahn, J. Y Lee, Int. J. Hydrogen Energy 16 (1991) 93.
[18] H. Oesterreicher, J. Clinton, H. Bittner, Mater. Res. Bull. 11 (1976) 1241.
[19] G. Alefeld, J. Volkl, in: Topics in Applied Physics, Vol. 29, Springer–Verlag, Berlin, Heiderberg, New York, 1978, p. 209.